A Trotting Horse Model

Hugh M. Herr and Thomas A. McMahon

The International Journal of Robotics Research 2000 19: 566
DOI: 10.1177/027836490001900602

A Trotting Horse Model

Hugh M. Herr

The Leg Laboratory
Massachusetts Institute of Technology
545 Technology Square, NE43-006
Cambridge, Massachusetts 02139, USA

Thomas A. McMahon

Division of Engineering and Applied Science
Harvard University
Pierce Hall 322
Cambridge, Massachusetts 02138, USA

Abstract

A new control strategy is used to stabilize numerical simulations of a horse model in the trotting quadrupedal gait. Several well-established experimental findings are predicted by the model, including how stride frequency and stride length change with forward running speed. Mass is distributed throughout the model's legs, trunk, and head in a realistic manner. Leg and trunk flexion is modeled using four flexible legs, a back joint, and a neck joint. In the control model, pitch stabilization is achieved without directly controlling body pitch, but rather by controlling both the aerial time and the foot speed of each stance leg. The legs behave as ideal springs while in contact with the ground, enabling the model to rebound from the ground with each trotting step. Numerical experiments are conducted to test the model's capacity to overcome a change in ground impedance. Model stability is maximized and the metabolic cost of trotting is minimized within a narrow range of leg stiffness where trotting horses of similar body size have been observed to operate. This work suggests that a horselike robot will exhibit behavior that is mechanically similar to that of a trotting horse if it operates in a narrow range of leg stiffness and employs simple control strategies where postural stabilization is an emergent property of the system.

KEY WORDS—horse, trotting, control, stability, ground impedance

1. Introduction

The investigation into quadrupedal locomotory control first began in 1893 when Lewis A. Rygg patented a mechanical horse (Rygg 1893). In his design, the horse stirrups were replaced by bicycle pedals that could be used by the rider to power the stepping motions of walking. The pedals were coupled to the limbs by a series of gears and linkages, such that each turn of the pedal crank consistently produced the same stepping motions. Rygg's approach to the control of a legged machine was not unlike other investigators of his time (Lucas 1894). In fact, similar locomotory models and mechanisms were proposed well into the 20th century, but their capacity to compensate for speed changes and environmental disturbances was poor (Nilson 1926; Ehrlich 1928; Kinch 1928; Snell 1947; Urschel 1949; Corson 1958; Bair 1959; Morrison 1968).

Beginning in the 1930s and continuing into the 1980s, researchers became increasingly convinced that for legged machines to be as agile and stable as legged animals, they must actively balance (Manter 1938; McGhee and Kuhner 1969; Frank 1970; Vukobratovic and Stepaneko 1972; Vukobratovic 1973; Gubina, Hemami, and McGhee 1974; Miura and Shimoyama 1980, 1984; Raibert 1985, 1986, 1990). Researchers believed that the fixed limb trajectories found in mechanisms of the past were the primary cause of their dysfunction and that feedback control should be used to balance a legged machine over its feet, similar to how a person balances a broom stick on the end of his or her finger. This view of legged control was so pervasive in the scientific community that the inverted pendulum model in walking became the primary tool for studying balance in legged locomotion (Miura and Shimoyama 1984; Vukobratovic and Stepaneko 1972; Vukobratovic 1973).

Marc Raibert and colleagues at MIT developed light and fast robots using the active balance approach to legged machine control (Raibert 1985, 1986, 1990). They built several robots, from a monopod to a quadruped, that could hop, run, jump, and flip. All the machines kept their balance actively; during ground contact, a gyroscope was used to measure errors in body posture, and then torques were applied about the joints to correct for the errors.

The International Journal of Robotics Research
Vol. 19, No. 6, June 2000, pp. 566-581,

In the late 1980s, Tad McGeer questioned the active balance paradigm as a control scheme for legged locomotion. He argued that legged machines should be designed with structures that are naturally stable, not requiring feedback of body posture during ground contact to balance (McGeer 1989, 1990). He built a passive robot that could walk down slopes driven by the force of gravity while balancing on curved feet shaped like the base of a rocking chair. After McGeer's work, Robert Ringrose built a hopping monopod robot that could bounce repeatedly in a stable limit cycle without relying on sensory input of posture to balance (Ringrose 1997). However, similar to McGeer's walking robot, the monopod's stability depended on the shape of its foot. Ringrose used a curved foot roughly the shape of a hemisphere. If the foot was made too flat or too small, the robot would fall over. Ringrose went on to show in simulation experiments that bipeds and quadrupeds could also use feet shaped like hemispheres to run, trot, and gallop without sensory input from the environment.

The legged machines described thus far, although functional in some sense, were not designed to resemble the shapes and motions of real animals. Raibert's quadrupedal robot did not include a head or a neck, or even a joint for the back to flex (Raibert 1985, 1986, 1990). Mechanically, the robot bounced a great deal during a trot, resulting in peak leg strains nearly twice as large as the strains measured in trotting animals of similar size and speed (Raibert 1986; Farley, Glasheen, and McMahon 1993).[1] The robots of McGeer and Ringrose, although compelling from an engineering perspective, are difficult to interpret as biological models simply because animals do not have large hemispherical feet or curved rocker feet. Many mammals run on their toes, not relying on a foot of any kind to maintain their balance (Biewener 1989; Roberts et al. 1997).

Do animals remain balanced while trotting by actively controlling body posture throughout ground contact, or are they naturally stable because of an inherently stable body shape? The purpose of this work is to begin to understand what control mechanisms quadrupeds use to maintain their speed, height, and balance while trotting. A goal for this paper is to develop a new theory of quadrupedal locomotory control and to use the theory to stabilize numerical simulations of a trotting horse model. We hypothesize that for robots to exhibit behavior that is mechanically similar to that of trotting horses, actively controlling body posture during stance is not necessary, not because of foot shape, but because of simple control strategies for which postural stabilization is an emergent property of the system. To test the hypothesis, a horse model is constructed using body segment lengths and mass distributions measured from a horse. Control strategies are then formulated using limb kinematic and force data from trotting animals. Quantitative predictions made by the model are compared to mechanical and energetic data from trotting horses.

1. Data from a trotting dog (23.6 Kg) was used from Farley, Glasheen, and McMahon (1993) to compute a peak leg strain of 14%. In contrast, Raibert's quadrupedal machine (25.2 Kg) bounced in trotting with leg strains around 25% (Raibert 1986).

2. Methods

2.1. Horse Model Structure

A considerable amount of mechanical and energetic data have been collected on small horses with a total body mass between 130 and 140 Kg (Alexander 1977; Hoyt and Taylor 1981; Heglund and Taylor 1988; Farley, Glasheen, and McMahon 1993). To construct the model proposed in this paper, morphological data were used from horses close to this size range, so that sufficient experimental evidence regarding horse dynamics and energetics would be available to test model predictions. Thus, a horse weighing 135 Kg with a mean leg length of 0.75 m served as a template for the model. These horse data were reported in Farley, Glasheen, and McMahon (1993) where high-speed video (200 frames/second, 16-mm video camera) was used to compute the leg length by taking the average of the forelimb and hindlimb lengths at first contact in trotting. They measured the forelimb length as the distance from the foot to a point midway between the greater tubercle and the dorsal aspect of the scapula, and the hindlimb length as the distance from the foot to the greater trochanter of the femur.

The horse model, shown in Figure 1, was formed by a series of rigid bodies connected by joints. Motions were confined to the saggital plane. Yaw and roll body motions were ignored. Each leg was constructed with an upper segment and a lower segment connected by a telescoping joint that allowed for sliding movement between the segments. Shoulders and hips were formed using pin joints, enabling each limb to retract and protract in the saggital plane.[2] Three separate segments were used for the rump, body, and neck/head, and back and neck pin joints were included to model trunk and neck flexion in trotting. The back joint was placed halfway between the tail base and the distal aspect of the rib cage where spine flexion is the greatest (Alexander 1985).

Mass was distributed between the legs, body, neck, and head in a realistic manner using morphological data from the literature (Fedak, Heglund, and Taylor 1982). This data set included the masses and moments of inertia of various body segments for a horse of total mass 98.9 Kg. To scale the mass segments from the smaller to the larger horse, it was assumed that corresponding body segments were the same fraction of total body mass.

2. Unfortunately, there is no accepted convention to describe the motions of the vertebrate limb as a whole. To avoid confusion, the convention proposed by Gray (1968) will be adopted throughout this paper. Any backward displacement of the foot toward the quadruped's rump, by means of rotating a limb about the hip or shoulder joint within the sagittal plane, will be referred to as limb retraction. Any forward foot displacement toward the quadruped's head will be described as limb protraction.

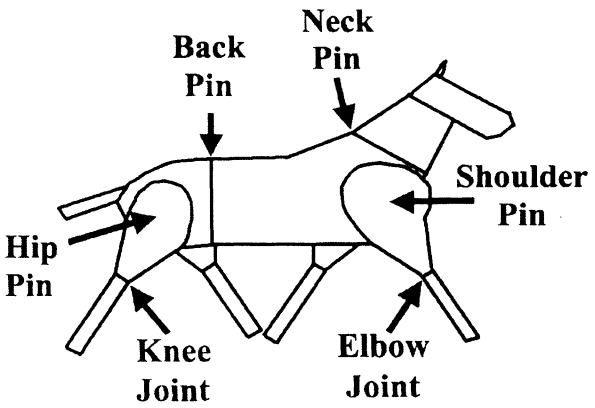

Fig. 1. The horse model used for the study is shown with the various leg, neck, and back joints noted. There are a total of 10 degrees of freedom, two per leg as well as a back joint and a neck joint. Telescoping joints at the knees and elbows allow the leg lengths to change. At the distal end of each leg is a single ground contact point. The ground is modeled as a field of linear springs and dampers that compress when the trotting model strikes the ground.

Joint locations and segment lengths were measured from the horse photographs of Muybridge (1979). The back flexion point, the shoulder to hip distance, the neck/head lengths, the shoulder to elbow distance, and the hip to knee distance were all measured from the images and normalized to leg length.[3] These dimensionless sagittal-plane lengths were then multiplied by the animal's leg length. The lateral thicknesses of the trunk, neck, and limbs were computed using the mass of each segment, the sagittal plane lengths, and the volume formula for each segment shape.

The ground was represented with linear springs and dampers in the vertical and horizontal directions to model the viscoelastic properties of a natural running surface. Ground stiffness was first set so that the limbs only penetrated the ground by a small amount when running ($\sim$ 0.3 cm). Increasing damping from zero then minimized oscillations between the ground and foot.

A compliant ground was required so that each model foot would not slip at first ground contact. The vertically aligned ground springs allowed each foot to penetrate the running surface, enabling the horizontal ground springs to hold the foot in place. The effect of ground impedance on model stability is discussed in Section 2.4 of the Methods section.

3. The back flexion point was measured by estimating the midway point between the tail base and the distal aspect of the rib cage. The shoulder-to-hip distance was measured from a point midway between the greater tubercle and the dorsal aspect of the scapula, and the greater trochanter of the femur. The distance from the elbow to the shoulder point and the distance from the knee to the hip point were also measured from the photograph.

2.2. Justification of the Control Methods

Trotting is typically described as an alternate gait in which a given pair of diagonal limbs (e.g., left fore and right hind) supports the body in every other contact period. Trotting is also described as a synchronous gait because a forelimb and its diagonal hindlimb are said to strike the ground at the same time. However, this is not always the case. When high-speed films of trotting are examined, it becomes apparent that sometimes the forelimb strikes the ground before the hindlimb, and at other times the hindlimb strikes the ground before the forelimb. This behavior is shown in Figure 2. The limb angles of a small trotting dog are plotted showing the forelimb striking the ground before the hindlimb. Figure 2 also shows that when the forelimb begins to retract, the hindlimb begins to retract even though the hindlimb is not in contact with the ground. Hence, both diagonal limbs begin retraction at the same time, and a limb sometimes begins to retract even before striking the ground.

Does the mechanical state of the animal trigger the retracting limb movement, or is the movement triggered by a clock or central pattern generator? It is unlikely that limb retraction begins when the first limb strikes the ground, since the time delay between detection of ground contact and the initiation of muscle force would cause the limb that is not in contact with the ground to begin retraction after its on-ground limb partner. If both limbs did not retract at the same time, the limbs would be nonparallel or skewed throughout stance, which is not what is observed (see Fig. 2).

An important hypothesis of the control model is that a trotting animal estimates when its limbs will first strike the ground using force and pitch information gathered during a previous stance period. This estimated time is then used to define when the limbs should first retract. The manner in which the time of retraction is computed is discussed in Section 2.3 of the Methods section.

Once an animal has made contact with the ground, how do the limbs, back, and neck respond? In 1977, Cavagna, Heglund, and Taylor discovered that in running, fluctuations in the forward kinetic energy of the center of mass are in phase with changes in the gravitational potential energy during ground contact. They hypothesized that animals most likely store elastic strain energy in tendon, ligament, and perhaps even bone to reduce fluctuations of total mechanical energy during a running step. In 1997, Roberts et al. found experimental evidence supporting that hypothesis. With direct measurements of force and length in a prominent ankle extensor of a running turkey, they showed that most of the length change during stance occurred in the tendon, not in the muscle fibers.

The idea that a vertebrate limb behaves like a spring during ground contact is an important feature in the McMahon and Cheng model that describes the mechanics of symmetric running gaits such as quadrupedal trotting and bipedal

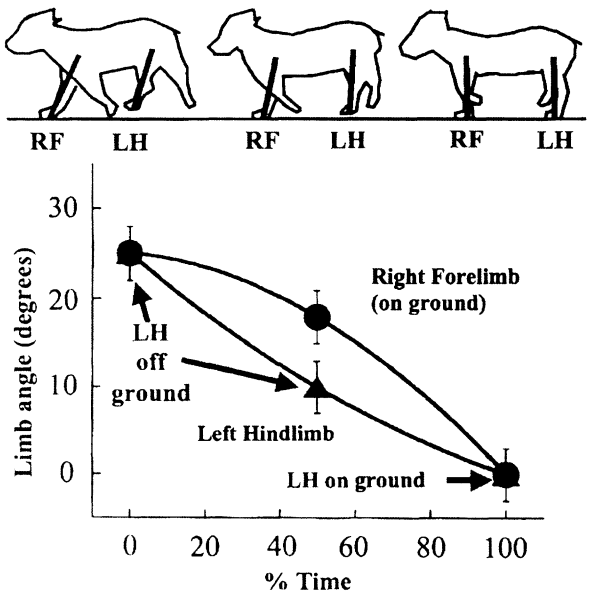

Fig. 2. The limb angles of a small trotting dog (5 Kg) are plotted against the percentage time between when the forelimb first makes contact with the ground and when the diagonal hindlimb makes contact. The circles correspond to the forelimb angle with respect to the vertical, and the triangles to the hindlimb angle. At 0% time, the forelimb first makes contact with the ground, but the hindlimb still has not made contact even though the fore- and hindlimb angles are the same. This is the situation in the left-hand drawing of the trotting dog. In the middle drawing at 50%, the same situation exists, except the aerial hindlimb has retracted toward the ground. Finally, at 100%, both legs are on the ground as shown in the right-hand drawing. The limb angles were measured using a video camera operating at a rate of 30 frames/second.

running (McMahon and Cheng 1990). The model predicts limb excursion angle and stride length by representing a limb as a simple spring. Similar to the McMahon and Cheng model, the horse model of this study uses efficient back, neck, and leg springs to rebound from the ground during each running step.

If the limbs of a quadruped behave like passive springs, where does the energy come from to sustain forward momentum in running?[4] A comparison of the musculature of quadrupedal hindlimbs and forelimbs provides some insight into this question. The preponderance of muscle mass in the hindlimb is positioned about the hip joint, acting to retract the hindlimb and to power a running step (Gray 1968). In distinction, a large fraction of forelimb muscle mass is positioned to protract the forelimb and to retard a running step. In Figure 3, hip and shoulder torques calculated using force-plate and video measurements applied to a small trotting dog are plotted against percentage contact time (Roberts 1997). The results show that the hip generally applies a thrusting torque and the shoulder a braking torque during contact in this trotting animal. A hypothesis in the trotting controller advanced here is that even in constant-speed running, hip torques act as the engine of quadrupedal trotting and shoulder torques as the brake.

2.3. Formulation of the Control Model

The control methods that dictate the motions and stiffnesses of the model's limbs in trotting may be summarized with a few simple rules. Although simple, the methods nonetheless lead to a robust stability and an overall model behavior consistent with what is known about the mechanics of quadrupedal trotting.

In Figure 4, the control strategy for trotting is explained using a series of model images at various stages in a running sequence. During the aerial phase of trotting, shown in Figures 4a and 4b, the controller positions the hip, shoulder, back, and neck to desired angular positions relative to the model's trunk. The leg lengths of a protracted limb pair are brought to full leg extension for landing, and the leg lengths of a retracted pair are shortened by a fixed amount to achieve foot clearance. The controller also computes when the limbs will contact the ground, given force and pitch information gathered during a previous stance period. At this estimated time of contact, two control commands are initiated. The controller switches to linear springs in the back and neck, as well as in the knee and elbow of the protracted limb pair. In addition, torques are

4. If a legged robot were constructed with only passive springs at its joints, flat-level running could be sustained for only a short time. Frictional losses would diminish the total mechanical energy of the robot with each running step, causing a rapid decay in the machine's forward speed and height. Even without frictional losses, the robot's actuators would have to perform mechanical work to accelerate and decelerate the machine's segments throughout a running cycle. A complete discussion of model energetics is given in the Discussion section.

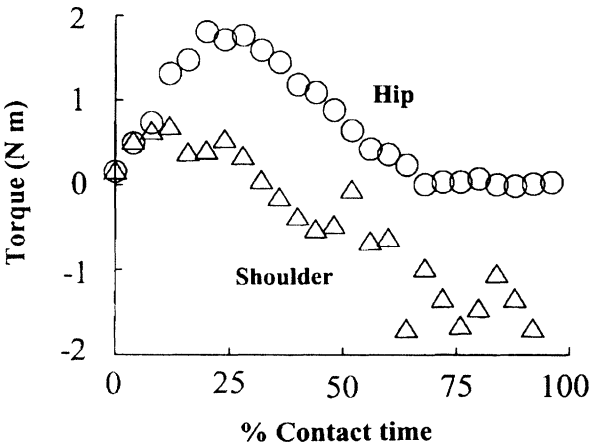

Fig. 3. The hip torque (circles) and shoulder torque (triangles) are plotted against percentage contact time for a small 5 Kg trotting dog. During ground contact, the muscles about the hip thrust the animal forward (positive torque), but the muscles about the shoulder generally retard forward motion (negative torque). The torques were computed by multiplying the force acting on a limb from the ground by the perpendicular distance from the line of force to the approximate axis of rotation of a joint. The ground reaction force was measured with a force platform, and the moment arm was measured by digitizing video records of the trotting dog. A 200 frames/second cine camera (photosonics 1PL) and a strain gauge force platform (model OR6-5-1, Advanced Mechanical Technology, Newton, MA) were used in the study. All animal points were calculated from experimental results given by Roberts (1997).

applied about the hip and shoulder of the protracted limbs to sustain the tangential velocity component of each foot measured relative to each foot's proximal hip or shoulder joint. Throughout stance,[5] this velocity control is then continued, as is shown in Figures 4c and 4d, until each foot loses contact with the ground.

In the aerial phase of trotting, conventional proportional-derivative (PD) servos are used to position the hip, shoulder, back, and neck joints to desired angular positions relative to the model's trunk. PD servos are also used to lengthen the limbs for landing and to shorten the limbs for foot clearance. To position a rotary pin joint, the PD servo takes the form

$$\text{Torque} = -G_p(\theta_m - \theta_t) - G_v(V_m - V_t), \qquad (1)$$

where G_p and G_v are position and velocity gains, and θ_m and θ_t are measured and target joint positions, and V_m and V_t are measured and target joint velocities, respectively. To position linear joints such as the knee or elbow, a force is applied to the joint proportional to linear position and velocity. For all the PD controllers, the target velocity is set to zero.

At the start of each aerial phase, the controller computes a delay time defined as the time separating the start of the aerial phase to the start of limb retraction. Since limb retraction should begin approximately when the model first strikes the ground, the delay time is an estimate of how long the model will remain in the air, or

$$T_{\text{delay}} = \frac{G_1 v}{g} + G_2(\hat{a}_{\text{prev}} - \hat{a}), \qquad (2)$$

where G_1 and G_2 are gains, v is the vertical take-off velocity of the model's center of mass measured at the beginning of the aerial phase, g is the gravitational constant, and $\hat{a}_{prev} - \hat{a}$ is the difference between the body pitch measured at the beginning of a previous aerial phase and the body pitch measured at the beginning of the current aerial phase. If G_1 is equal to two, the first term on the right-hand side of eq. (2) is an estimate of the aerial time for a ballistic point mass moving in a uniform gravitational field with a starting vertical velocity equal to v. The second term on the right-hand side of eq. (2) modifies the ballistic estimate of aerial time when model pitch is changing from one trotting step to the next. For example, if body pitch is gradually increasing, the aerial time or delay time will be reduced from the ballistic point mass estimate by an amount proportional to the difference in pitch from one step to the next.

The vertical take-off velocity, v, in eq. (2) is computed by integrating the total vertical force, F_v, acting on the model's legs during ground contact, or

$$v = \frac{1}{2}\left(\frac{\int_0^{t_c} F_v dt}{m} - g t_c\right), \qquad (3)$$

where m is the total body mass and t_c is the amount of time the limbs are in contact with the ground.

To control forward running speed, torques are applied about the hip and shoulder such that the tangential velocity component of each foot, measured relative to each foot's proximal hip or shoulder joint, is sustained. Foot velocity is computed by multiplying the leg length, l, by the angular velocity of the proximal hip or shoulder joint measured relative to the trunk, $\dot{\theta}$, or

$$V_{\text{tang}} = l\dot{\theta}. \qquad (4)$$

The applied torque is then proportional to the difference between a measured tangential velocity component and a target velocity, or

$$\text{Torque} = -G_v(V_{\text{tang}} - V_{\text{target}}). \qquad (5)$$

The proportionality constant, G_v, is a velocity gain defining the torque response to a given velocity error.

5. Occasionally, a model foot "chatters" or bounces momentarily off the ground. Regardless of whether foot chatter occurs or not, the same stance control is initiated when a limb first contacts the ground in a protracted or forward position.

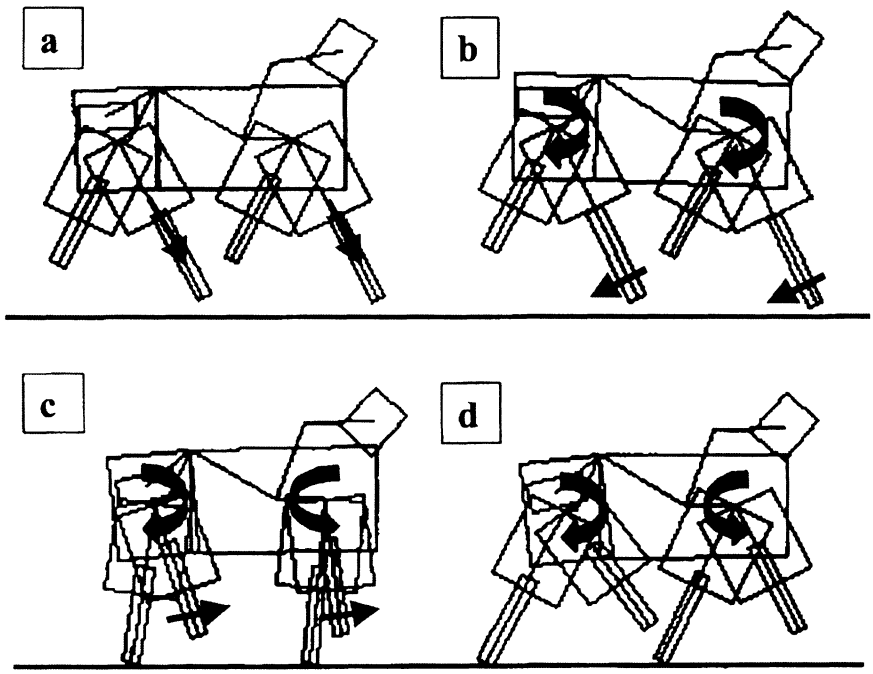

Fig. 4. The horse model is sketched in a trotting sequence. In (a), when the legs are off the ground, the controller positions one diagonal limb pair at a backward or retracted angle with respect to the trunk and the other pair at a forward or protracted angle. The lengths of the protracted limbs are then positioned to full extension for landing, and the retracted pair are shortened to fixed lengths for foot clearance. The back and neck joints are positioned to desired angular positions in preparation for landing. At the beginning of the aerial phase, the controller also computes when the limbs will contact the ground, given force and pitch information gathered during a previous stance period. At this estimated time of contact, two control commands are initiated. First, the knee and elbow joints of the protracted limbs, as well as the back and neck joints, are stiffened in preparation for ground contact. Second, the controller exerts torques about the protracted hip and shoulder joints to sustain the tangential velocity component of each foot measured relative to each foot's proximal hip or shoulder joint. The velocity control then continues throughout stance, here sketched in (c) and (d). The tangential velocity component of each foot is computed by multiplying the leg length by the angular velocity of the proximal hip or shoulder joint measured relative to the trunk. The applied torque is proportional to the difference between the measured tangential velocity and a target velocity. When the target hindlimb velocity is greater than the forward running velocity, and the target forelimb velocity is less, a thrusting torque is applied about the hip and a braking torque about the shoulder as is shown in (c) and (d). This braking and thrusting behavior keeps the body pitch level during stance. When the model is in contact with the ground, linear springs act at the knee, elbow, neck, and back, enabling the model to rebound from the ground with each step.

When the forelimb target velocity is smaller than the forward velocity of the trotting model and the hindlimb target velocity is greater, the shoulder generally applies a braking torque during stance and the hip a thrusting torque similar to the trotting dog of Figure 3. This thrusting and braking behavior increases model stability by decreasing angular fluctuations in body pitch throughout stance. A full discussion of pitch control can be found in the Discussion section of this paper.

2.4. Simulation Experiments

Given the large number of degrees of freedom in the horse model, and the nonlinear nature of quadrupedal trotting, complete analytical solutions were not practical in this study. Instead, physically realistic computer simulations were used to study the forces and motions of trotting. The simulations obeyed the laws of Newtonian physics as applied to trees of rigid bodies coupled together by joints.

A commercially available modeling package called SD-Fast (Rosenthal and Sherman 1986) produced the simulation dynamics by generating the equations of motion and then solving them numerically using a fourth-order Runge-Kutta integration method. The equations were integrated forward at a fixed time step of 0.4 ms, while another program called Creature Library communicated with the controller and SD-Fast to determine the forces and torques commanded to the model's joints. Animation packages within the Creature Library made it possible not only to analyze the simulation results numerically but also to see them visually. This enabled the horse model to be tested not only on the basis of its predictive capability but also on how visually realistic the trotting simulations seemed.

The horse model was constrained to move in the sagittal plane during all numerical experiments. In this study, analysis was not performed to determine whether trotting was the better gait, by any criterion, at a particular running speed. Rather, published observations of animal velocities were used to define the full velocity range of trotting (Heglund and Taylor 1988). Four trotting velocities were examined, ranging from a slow trot at 2.1 meters/second to a fast trot at 4.4 meters/second.

2.4.1. Stability

The first task in numerical simulation was to find a stable trotting simulation at the lowest trotting speed, or 2.1 meters/second. This was accomplished by manually adjusting (1) positions and velocities that describe the initial state of the model; (2) the back, neck, and leg contact stiffnesses; (3) the position and velocity gains; and (4) the target positions and velocities. It was discovered that when the contact limbs were very compliant, with peak leg strains at mid-stance around 40%, the model's stability was very sensitive to the initial conditions of the simulation. When the sum of fore- and hindlimb stiffness was increased, this sensitivity to initial conditions disappeared. The ratio of forelimb to hindlimb stiffness was adjusted such that both limbs compressed by the same amount at mid-stance when both the pitch and pitch velocity were zero at first ground contact.

Stable trotting was found at 2.1 meters/second using a total leg stiffness, k_{leg}, equal to 24 kN/meter. Leg stiffness, k_{leg}, is defined in the appendix, eq. (A.1). Once a stable trotting simulation was achieved, parameters were further adjusted to minimize the mechanical work necessary to stabilize the trotting simulation during each running cycle. When the neck was made very stiff, the head would go through multiple oscillations during a single stance period, destabilizing the trotting motions. To correct this problem, neck stiffness was lowered until only a single neck oscillation would occur during each stance period. The same criterion was used to define the stiffness of the back during stance. The aerial position and velocity gains were also adjusted. The gains were lowered until the time required to position each joint was equal to the aerial phase time, and each limb moved to its target position with zero overshoot.

The aerial PD servo position and velocity gains and the back and neck contact stiffnesses, once defined at the lowest trotting speed, were not adjusted across the entire span of trotting from 2.1 meters/second to 4.4 meters/second. To find stability at different speeds, only the limb excursion angle at first ground contact and the fore- and hindlimb target velocities had to be adjusted at a given limb stiffness.

The effect of contact leg stiffness on model stability was examined after stable simulations were found at the four trotting speeds. Is there a critical leg stiffness range where model stability is maximized in trotting? To answer this question, the total limb stiffness, or k_{leg}, was incrementally increased at each speed while keeping the ratio of fore- and hindlimb stiffness constant. At each k_{leg} value, the limb excursion angle at first ground contact was minimized, because it was discovered that the smaller the limb angle, the smaller the vertical oscillations of the model's center of mass, and the lower the peak leg strain during stance. Another consequence of choosing the smallest angle was that the model's vertical stiffness, k_{vert}, was maximized. Vertical stiffness, k_{vert}, is defined in the appendix, eq. (A.2).

To measure the model's capacity to overcome a change in ground impedance, a numerical experiment was conducted at each trotting speed, limb excursion angle, and total limb stiffness, k_{leg}. In the experiment, ground impedance was reduced only after the model had been trotting on a stiff running surface[6] in a stable limit cycle. Once reduced, ground stiffness was not changed for the remaining time of simulation. With a small change to ground impedance, the model quickly

6. As noted in Section 2.1 of the Methods section, maximum ground penetration on the stiff surface was approximately 0.3 cm.

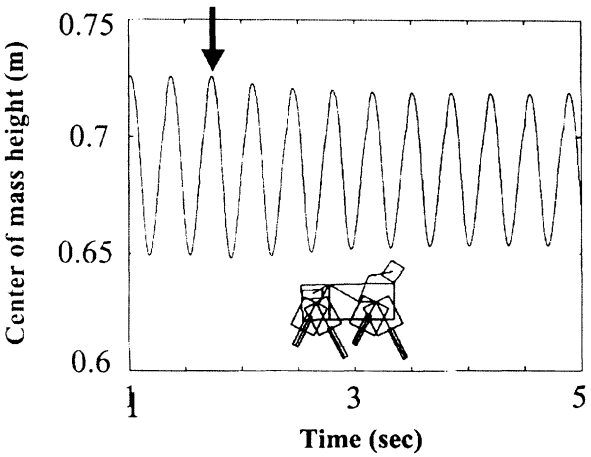

Fig. 5. The vertical height of the model's center of mass measured from the undeflected ground surface is plotted against time for a steady trot at 2.1 meters/second. The stiffness of the running surface was reduced by 30% from 400 kN/meter to 280 kN/meter at 1.7 seconds (denoted by arrow) at a point when the trotting model was off the ground. At 4 seconds, or three trotting cycles after the ground stiffness had been reduced, the trotting model found a new stable limit cycle. On the softer running surface, the model trotted with a higher stride frequency compared to the more rigid surface. After the ground disturbance, the simulation ran for another 20 trotting cycles without a significant change to maximum aerial height, body pitch, or forward velocity (least-squares regression, $P < 0.05$).

recovered from the disturbance. However, when ground impedance was decreased beyond a critical level, the model could not remain upright on the soft ground. In each experiment, the model was considered successful in overcoming a change in ground impedance if the model found a new stable limit cycle[7] on the softer running surface. An example of how the model responded to a change in ground impedance is shown in Figure 5.

2.4.2. Setting Stiffness Values

In an effort to define a leg stiffness range where the model exhibits an optimal stability characteristic, the largest percentage reduction in ground stiffness the model was able to overcome at each k_{leg} value was plotted against k_{leg} at each trotting speed. In Figure 6(a), the results are shown for the fastest trotting speed, or 4.4 meters/second. Model simulations with k_{leg} values between 24 kN m^{-1} and 40 kN m^{-1} showed the greatest capacity for overcoming changes in ground impedance. At this speed, horses have been shown to use k_{leg} values that fall within the shaded region of Figure 6(a), at the high-stability plateau. As shown in Figure 6(b), at the low stiffness end of the high-stability range, the model also predicted that the cost of transport, or the metabolic energy an animal consumes in moving a unit of body weight a unit distance, is minimized. The method used to estimate the cost of transport is described in the appendix.

It seems that animals operate near the low end of leg stiffness where metabolic energy is the lowest and where the stability characteristics of the model are most favorable. Hence, to make predictions of animal behavior at each trotting speed, leg stiffness values were taken from the high-stability region.

3. Results

3.1. Hip Thrusting and Shoulder Braking

During a trot, hip torques generally thrusted the model forward, powering a running step, and shoulder torques generally impeded forward progression. This behavior was a prevalent model characteristic in steady state running. Since the target forelimb velocity was less than the forward speed of the model, and the target hindlimb velocity was greater, the shoulder generally applied a braking torque and the hip a thrusting torque. As an example, when the average forward trotting speed was 4.4 meters/second, the forelimb target velocity was 3.5 meters/second and the hindlimb target velocity was 5.2 meters/second. Consequently, braking shoulder torques and thrusting hip torques were applied by the model's actuators. This antagonist/protagonist behavior minimized pitch fluctuations and increased model stability. A complete discussion of model stability is given in the Discussion section.

3.2. Overall Mechanics and Energetics of the Model

The model's leg stiffness, k_{leg}, and vertical stiffness, k_{vert}, were compared to experimental stiffness values measured by Farley, Glasheen, and McMahon (1993) on a horse of similar body size (135 Kg) and running at similar trotting speeds (2.1 meters/second to 4.4 meters/second). Animal stiffnesses, k_{leg} and k_{vert}, are defined in the appendix, eqs. (A.1) and (A.2), respectively. The model exhibited similar compliance behavior, shown in Figure 7a, as the small trotting horse. The leg stiffness, k_{leg}, changed little with forward trotting speed ($k_{leg} = 21.4 + 1.89v$), but the vertical stiffness, k_{vert}, increased dramatically ($k_{vert} = 83.5 - 42.9v + 12.9v^2$). To run faster, the horse model rebounded from the ground more quickly, exerting larger forces on the ground and increasing its vertical stiffness, k_{vert}. Similar to a running horse, the model achieved this force increase not by increasing leg stiffness, but

7. The model was considered to be in a stable limit cycle if trotting continued for 20 running cycles without a significant change to maximum aerial height, pitch, and forward velocity (least-squares regression, $P < 0.05$).

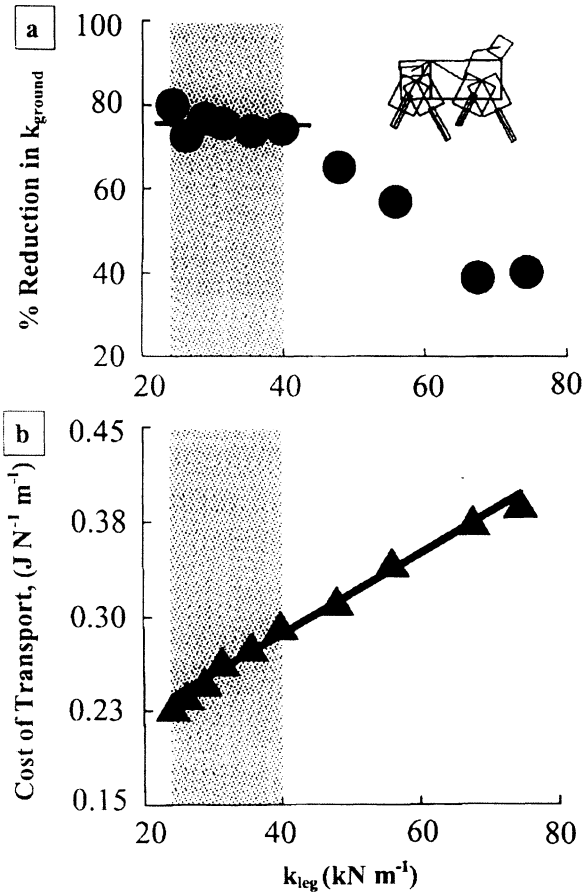

Fig. 6. The maximum percentage reduction in ground stiffness the trotting horse model could overcome in stability tests is plotted in (a) against the effective leg stiffness, k_{leg}, defined in eq. (A.1) of the appendix. At the highest trotting speed, horse simulations with k_{leg} values of 24 kN m^{-1} and higher exhibited the greatest ability to overcome disturbances in pitch. However, at this speed, a horse uses k_{leg} values within the shaded region, at the low-stiffness end of the stability region (Farley, Glasheen, and McMahon 1993). The reason for this low-stiffness preference by animals becomes evident when the metabolic cost of transport, plotted in (b), is examined at each k_{leg}. It seems that trotting horses use leg stiffnesses where they are highly stable but where energy expenditure is the lowest. The cost of transport is defined in the appendix.

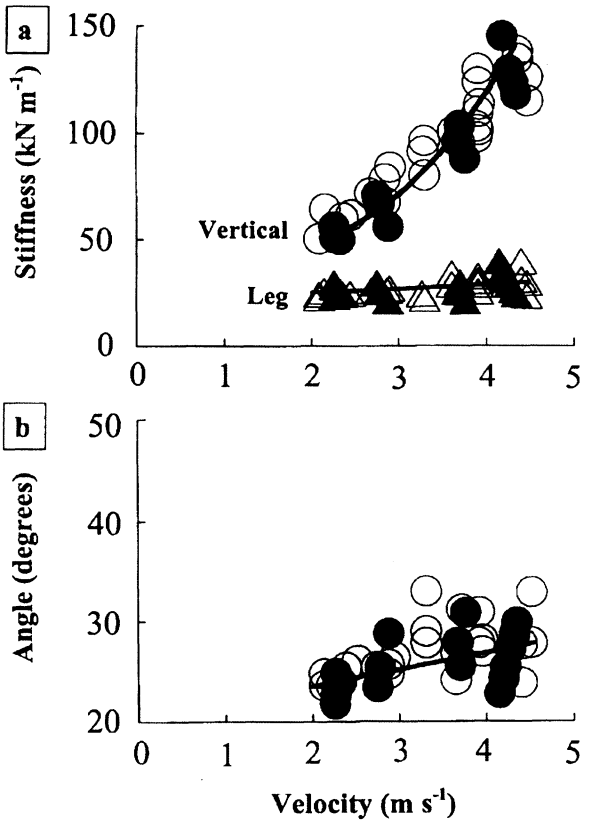

Fig. 7. In (a), leg stiffness, k_{leg}, and vertical stiffness, k_{vert}, are plotted against forward trotting speed. In (b), the limb excursion angle upon first ground contact, $\grave{e}_o$, is plotted against the same range of forward trotting speeds. In both plots, the open circles are animal data from a horse (135 Kg) adapted with permission from Farley, Glasheen, and McMahon (1993), and the closed circles are data from horse model simulations. The leg stiffness, k_{leg}, vertical stiffness, k_{vert}, and limb excursion angle, $\grave{e}_o$, are defined in McMahon and Cheng (1990) and also in the appendix, eqs. (A.1), (A.2), and (A.3), respectively. In (a) and (b), least-squares regression lines are fitted to the simulation data ($k_{leg} = 21.4 + 1.89v$; $k_{vert} = 83.5 - 42.9v + 12.9v2$; $\grave{e}_o = 20.2 + 1.65v$), showing good agreement with the experimental data.

by sweeping out larger limb excursion angles to increase the compression of its leg springs. In Figure 7b, the limb excursion angle, defined in the appendix, eq. (A.3), increased with increasing forward speed ($\dot{e}_o = 20.2 + 1.6v$), in agreement with experimental data.

Model stride frequency, the inverse of the total cycle time, was compared to experimental data taken by Heglund and Taylor (1988) on a small trotting horse (140 Kg). The results, plotted in Figure 8a, agree with the running horse data. Stride frequency increased with trotting speed with a slope of 0.3. The model's stride length, normalized by leg length, was compared to experimental observations on horses, large cats, dogs, a man, a rhea, and an ostrich presented by Alexander (1977) and McMahon and Cheng (1990) (Figure 8b). Relative stride length increased with forward Froude number, a dimensionless velocity, in a manner similar to the running bipeds and quadrupeds.

The model's cost of transport was computed and then compared to the cost of transport of a small running horse (140 Kg) measured in the study of Hoyt and Taylor (1981). The model results, plotted in Figure 9, showed excellent agreement with the horse data. The Kram and Taylor rule (1990) was used to estimate the cost of transport using only the model's forward running speed and average limb contact time in steady state running. A cost coefficient, C_o, was also used to estimate the model's cost of transport. The values used to estimate the energy consumption plotted in Figure 9 are listed in Table 1. The cost coefficient values were adjusted until the simulation data agreed with the empirical data of Figure 9. In Table 2, experimental measurements of the cost coefficient, C_o, made by Kram and Taylor (1990), are listed for three trotting speeds. The cost coefficient values in Table 1 agree well with the experimental values listed in Table 2. The manner in which the cost of transport was computed is discussed in the appendix.

4. Discussion

4.1. Legged Machine Control

Legged machines have balanced successfully while walking and running using one of two control strategies. In one strategy, machines remained upright by actively balancing

Table 1. Cost Coefficient Values Used to Estimate the Model's Cost of Transport (Figure 9) Are Listed at Four Trotting Speeds (T)

Forward Speed (meters/sec)	Cost Coefficient (Joules/Newton)
2.1 (T)	0.154
2.7 (T)	0.156
3.6 (T)	0.167
4.4 (T)	0.173

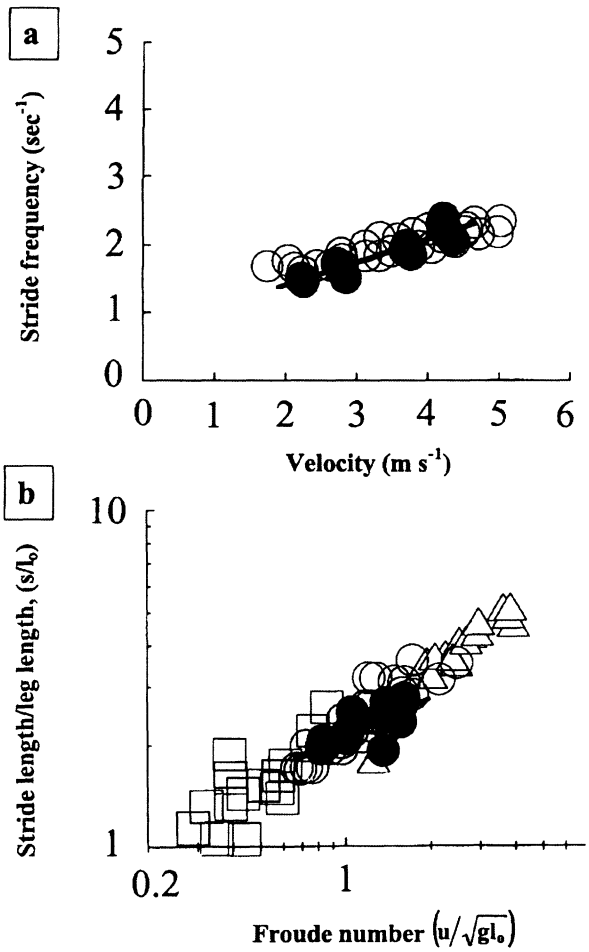

Fig. 8. In (a), stride frequency is plotted against forward speed. Here, stride frequency = $1/T$, where T is the time between footfalls of the same foot. Open circles are animal data from a trotting horse (140 Kg), adapted with permission from Heglund and Taylor (1988), and closed symbols are simulation results. Least-squares regression lines are fitted to the simulation data ($f_{\text{trot}} = 0.7 + 0.34v$), showing qualitative agreement with the experimental data. In (b), the distance the horse model moved in one complete trotting cycle, or the stride length, s, is normalized by the leg length, l_o, and plotted on logarithmic coordinates against the forward Froude number, $U = u/\sqrt{gl_o}$, where u is the forward velocity and g the gravitational constant. Once again, the open symbols are animal data and the closed symbols are simulation data. A least-squares regression line is fitted to the trotting simulation data ($s/l_o = 2.1U^{0.4}$), in general agreement with the experimental data. The squares are walking stride lengths, the circles trotting, and the triangles galloping. Animals represented include horses, large cats, dogs, man, a rhea, and an ostrich. Animal data adapted with permission from Alexander (1977) and McMahon and Cheng (1990).

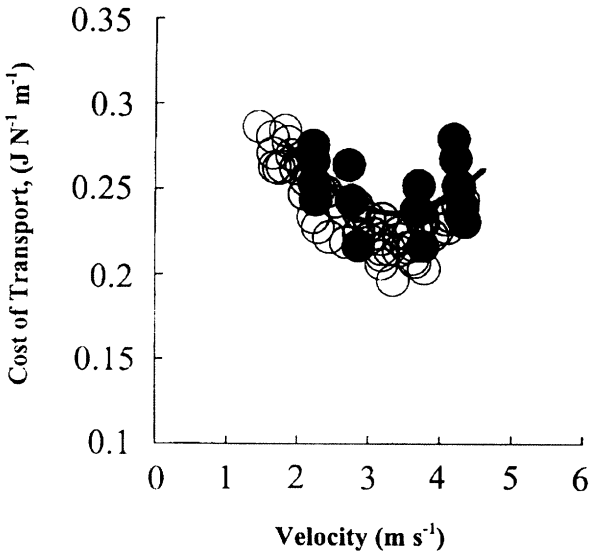

Fig. 9. The cost of transport, or the metabolic energy consumed by a trotting horse in moving a unit of body weight a unit distance, is plotted versus speed for the running model (135 Kg, filled symbols) and a running horse (140 Kg, open symbols). The experimental horse data were taken with permission from Hoyt and Taylor (1981). The Kram and Taylor rule (1990) was used to estimate the cost of transport for the model, using the model's forward running speed and average limb contact time in steady-state running. Experimental measurements of the cost coefficient, C_o, made by Kram and Taylor (1990), were also used at each running speed. These values are listed in Table 2. The manner in which the cost of transport was computed is discussed in the appendix.

Table 2. At Three Trotting Speeds (T), Cost Coefficient Values Are Listed

Forward Speed (meters/sec)	Cost Coefficient (Joules/Newton)
2.0 (T)	0.154 ± 0.024
3.0 (T)	0.166 ± 0.014
4.0 (T)	0.173 ± 0.012

NOTE: Standard errors of the mean are included for four small horses (mean body mass = 141 Kg). Adapted from Kram and Taylor (1990); reprinted with permission.

(Manter 1938; McGhee and Kuhner 1969; Frank 1970; Vukobratovic and Stepaneko 1972; Vukobratovic 1973; Gubina, Hemami, and McGhee 1974; Miura and Shimoyama 1980, 1984; Raibert 1985, 1986, 1990). During ground contact, a gyroscopic sensor typically was used to detect errors in a machine's spatial orientation, and actuator forces were then applied to minimize these errors. In a second strategy, machines relied on large curved feet to ensure their balance rather than active control systems (McGeer 1989, 1990; Ringrose 1997). In this strategy, a machine was stable simply because of its shape, requiring no sensory information from the environment whatsoever.

Although quadrupedal machines were stabilized using these control strategies (Raibert 1985, 1986, 1990; Ringrose 1997), they nonetheless did not specifically resemble running animals, morphologically or dynamically. Little is known about how horses, or for that matter animals in general, balance when running. However, since quadrupedal animals do not have large curved feet to ensure their balance, researchers have speculated that they must actively balance to remain upright, most likely relying on their vestibular system instead of a gyroscope for sensing postural orientation (Raibert 1986). In the present study, we examined how a horselike robot could achieve a stable body pitch and forward speed in running. We used a numerically simulated horse model to test different control strategies. This study represents a first attempt at understanding how quadrupedal animals might stabilize their movement in trotting, even without the use of vestibular inputs to actively balance during ground contact.

4.2. Does a Horselike Robot Have to Actively Balance When Trotting?

Our findings support the hypothesis that a horselike robot does not have to actively balance to remain upright from running cycle to running cycle. In the model, body pitch is not directly controlled to correct for errors in pitch during ground contact. Rather, pitch stabilization is achieved indirectly by controlling when each foot begins to retract toward the ground during the aerial phase, and how fast each stance foot moves relative to the model's trunk during ground contact. Sensory knowledge

of body pitch is not used to actively balance the model but only to modulate when the limbs begin to retract toward the ground. Interestingly, when only vertical force information is used to modulate retraction time, excluding pitch information, the model has no difficulty remaining balanced. However, when pitch information is excluded, the trotting motion is irregular and not smooth. The model bounces to different heights from one running cycle to the next, exhibiting a pulsing behavior in time where bouncing height increases to a maximum and then decreases to a minimum and then increases again, and so on, in a systematic manner. When pitch information is employed, the bouncing height becomes steady and regular. This result suggests that a horse may employ body pitch information to make trotting smoother, not specifically to remain balanced in steady state trotting.

4.3. Does Foot Shape Enhance the Stability of the Model?

The model does not require large curved feet to remain balanced from running cycle to running cycle. In fact, the model does not even have feet. Each limb contacts the ground at a single point, making the model statically unstable. The horse model uses a controller to remain upright, requiring the following sensory information: (1) ground reaction forces applied to each limb, (2) the angle and velocity of each limb, (3) the leg length and the time rate of change of leg length, and (4) back and neck joint angles.

4.4. How Does the Horse Model Remain Balanced without Directly Controlling Body Pitch?

By sustaining the tangential velocity component of each foot measured relative to a proximal limb joint, the controller effectively maintains forward speed. But this velocity control also has a stabilizing effect on body pitch. When the forelimb target velocity is smaller than the forward velocity of the trotting model and the hindlimb target velocity is greater, the shoulder generally applies a braking torque during stance and the hip a thrusting torque similar to the trotting dog of Figure 3. This thrusting and braking behavior increases model stability by decreasing angular fluctuations in body pitch throughout stance, keeping the trunk parallel to the ground without sensory knowledge of the trunk's orientation in space.

In a trot, if an error in pitch causes the hindlimb to strike the ground before the forelimb, the thrusting hip counters the gravitational and inertial forces tending to nose the model into the ground. On the contrary, if the forelimb strikes first, the braking shoulder counters the gravitational and inertial forces tending to push the hip lower than the shoulder. By adjusting the hind and forelimb target velocities, forward velocity is stabilized and errors in body pitch are diminished during stance, with the hips acting as the engine of trotting and the shoulders as the brake.

Also critical to pitch stabilization is the fact that both protracted diagonal limbs retract toward the ground at the same time, before actually striking the ground, near the end of the aerial phase. A consequence of this control is that both limbs remain approximately parallel throughout stance, tending to keep the model's trunk level with the ground. If limb retraction only began after a foot actually struck the ground, and if an error in body pitch caused one foot to strike the ground before the other foot, the limbs would not be parallel with one another at mid-stance. This would be true simply because the second limb to contact the ground would not begin its retraction at the same time as the first contact limb. By the time the second limb touched down, the first limb would have retracted a great deal, causing the limbs to be skewed throughout stance. Since the limbs are not parallel, one limb would leave the ground before the other limb, destabilizing model pitch.

4.5. How Is the Total Hip/Shoulder Positive Work Dissipated?

Positive mechanical work has to be supplied by the model's actuators to sustain forward trotting momentum. There are two cases in which negative work is performed on the running model. Nonconservative forces from linear dampers in the ground diminish the model's mechanical energy with each running step. In addition to ground losses, the model's actuators perform negative work to decelerate body segments throughout each running cycle. Both the negative work from ground dampers and, more significantly, the negative actuator work required to decelerate body segments must be "paid for" by positive hip/shoulder actuator work for the total mechanical energy of the running model to be nearly periodic. In simulation experiments, 160 Joules of work from hip/shoulder actuators were required to sustain forward trotting momentum at 4.4 meters/second. Of this energy, only 5% was lost to ground dampers while the remaining energy went into decelerating model segments throughout the trotting cycle.

4.6. Why Is Leg Length Critical in Speed Control?

By keeping the tangential velocity component of each foot constant relative to a proximal limb joint, the forward speed of the horse model is effectively controlled in trotting. But why control tangential foot velocity and not angular velocity of the limb? In some sense, the controller attempts to move the limbs as if they were spokes of a steadily rolling wheel, forcing each foot to move in a steady manner similar to a wheel's rim. However, unlike conventional wheels with rigid spokes, the legs are compliant and may change length. If two vehicles are traveling at the same forward speed, but one vehicle has large wheels and the other has small wheels, the small wheels will rotate at a higher angular velocity. Similarly, when the model strikes the ground with an unusually large downward velocity,

the legs compress more, causing them to rotate faster for a given forward running speed. Thus, forcing angular velocity to be constant will not result in a steady forward velocity because compliant legs may change length from one running cycle to the next.

4.7. How Plausible Is the Horse Model as a Biological Representation?

The plausibility of the horse model can be tested in a number of different ways. One test is whether the control methods lead to an overall model behavior that is consistent with the mechanics and energetics of trotting horses. In Figures 7 through 9, the simulation results show good agreement with experimental measurements on horses describing animal stiffness, limb excursion angle, stride frequency, relative stride length, and the metabolic cost of transport measured at four different trotting speeds. It is important to point out that the metabolic predictions of Figure 9 test both the horse model and the Kram and Taylor empirical rule introduced in the appendix, eq. (A.5). The horse model predicts how much time, on average, each limb spends on the ground in trotting, and the Kram and Taylor rule then makes a prediction of metabolic rate.

Limb-retraction movements of the trotting model agree qualitatively with animal behavior. In the control model, both protracted limbs begin retraction simultaneously, near the end of the aerial phase. Limb retraction is not triggered by first ground contact but at a computed time after the start of the aerial phase. With this control, a limb sometimes begins to retract before actually striking the ground. This model characteristic is similar to the limb motions of the trotting dog in Figure 2. At the end of the aerial phase, close to when the dog's forelimb first strikes the ground, both diagonal limbs begin to retract toward the ground at the same time, remaining nearly parallel even though the hindlimb contacts the ground after the forelimb.

Another test of model plausibility is whether the control inputs are consistent with what is known about biological sensing. The model's controller requires sensory information reporting ground reaction forces applied to each limb, the angle and velocity of each limb with respect to the body, the length and rate of change of leg length, back and neck joint angles, and body pitch.

Animals can measure a joint's position and velocity using sensory receptors at or around the joint, or in the muscle fiber that actuates the joint (Eyzaguirre and Fidone 1975). The most common receptor within a joint measures both position and velocity. In the absence of movement, the receptor signals the position of the joint, but during movement, its discharge shows a distinct velocity dependency. An animal can also measure a joint's position and velocity using stretch receptors called spindle organs located within muscle fiber (Eyzaguirre and Fidone 1975). A spindle organ is typically attached in parallel with the main muscle mass. Consequently, the organ experiences the same relative length change as the overall muscle, thereby acting as a muscle strain gauge.

To determine which limbs are on the ground during locomotion and the forces exerted on each limb, animals could use either cutaneous receptors in their feet or muscle force receptors. Animals can detect joint force by measuring the amount of tendon stretch in muscle-tendon units actuating a joint (Eyzaguirre and Fidone 1975). A tendon organ sends out action potentials that propagate toward the spinal cord with greater frequency when the tendon is actively stretched. Since tendon is in series with muscle, an increase in frequency also correlates with an increase in the force borne by the muscle fibers.

The vestibular system could be employed to measure body pitch. This information could then be used to effectively modulate the retraction time to make trotting smoother. The vestibular apparatus has been shown to be critical for the execution of many animal movements, such as when an animal gets up from lying on its side or righting itself in a free fall (Eyzaguirre and Fidone 1975).

Another model test is whether the torques applied at the model's hips and shoulders during stance could actually be applied by muscles of a horse. Clearly, the control scheme presented here could not be viewed as a realistic biological representation if, to achieve stability, the model's actuators had to provide moments greater than those obtainable from a horse's musculature. Hip and shoulder torques for the trotting model show peak values around 120 Nm for both the hip and shoulder. Is this torque value reasonable? When joint torques were measured on four healthy human males (Mean body mass = 78.7 Kg) by Roberts (1995), peak hip torque increased from 25 Nm to 120 Nm when subjects ran up increasingly steeper slopes from 0 to 12 deg. It seems reasonable that a running horse weighing 135 Kg would be capable of exerting torques about its hip and shoulder at least comparable to the hip torques of a human runner weighing only 78 Kg.

A final plausibility test is whether model stability is sensitive to ground impedance. When animals run in the natural world, they encounter ground surfaces with a wide variety of stiffnesses. Anyone who has ever played catch with a dog can testify that animals easily remain balanced when running from a rocky trail to a compliant grass surface. Without a single control parameter adjustment, the model trotted robustly when ground stiffness was reduced by almost 80% (from 660 to 126 kN/m; see best fitting line in shaded region, Fig. 6a).

4.8. Alternative Control Schemes

We investigated three alternatives to the control scheme of Figure 4, to see whether or not stable trotting might still be obtained. In one scheme, forward trotting speed was sustained by requiring both limbs to lengthen beyond their equilibrium length to thrust the model upward and forward at the end of

stance. A consequence of this control was that the vertical oscillations of the center of mass increased dramatically because the extending limbs exerted too great a vertical lifting force on the trunk. The gait resembled a bounding motion more than a trot, resulting in a vertical stiffness, k_{vert}, that was much smaller than what has been measured in trotting animals at a given leg stiffness, k_{leg} (see eqs. (A.1) and (A.2), in the appendix). The model made realistic predictions of gait parameters (shown here in Figs. 7 through 9) only when thrusting hip and shoulder torques sustained forward running momentum, and only when the stance legs behaved as ideal springs operating within a particular narrow range of stiffness.

In a second control scheme, both diagonal limbs began to retract at the instant of first ground contact of one or both diagonal limbs. This control strategy produced stable trotting simulations that made realistic predictions of experimental data (Herr 1998). However, when biologically realistic delay times of 80 ms or higher were used to set the time between actual foot strike and the initiation of limb retraction, the trotting simulation could no longer be stabilized. For this reason, this particular retraction strategy was not viewed as a realistic biological representation and was abandoned.

It was also discovered that if pitch was directly controlled, the model could run robustly without aerial limb retraction. When the control scheme was altered such that each limb began its rearward retraction at the instant of first ground contact and not before, pitch stabilization could only be achieved through the direct application of hip and shoulder torques to level the body during stance. This result suggests that limb retraction (as in the scheme of Fig. 4) not only brings the model into agreement with experimental observations but also enables the model to stabilize body pitch indirectly as an emergent property of the system.

5. Conclusions

The results of this study provide a conceptual framework for understanding the movements of a trotting horse, and how these movements change with speed. Furthermore, results presented here may lead to an improved quadrupedal trotting machine. We have demonstrated that a horse model based on ideal springs in the diagonal stance legs is capable of simulating most features of the trotting gait if leg stiffness falls within a particular narrow range (see Fig. 6) and if hip and shoulder torques sustain forward running momentum. The model made realistic predictions for the dependence on speed of important gait parameters, including stride frequency, stride length, and the cost of transport. Predictions were best when the model employed one of three control strategies where postural (pitch) stabilization results. One of the control strategies is given special attention in this paper because of its basis in biological evidence. In this strategy, pitch stabilization is not controlled directly. Instead, control of the aerial time and foot speed during stance was found to provide an automatic stabilization of body pitch.

Appendix: Relevant Background Information

The Mechanics of Trotting

Biologically motivated models of quadrupedal trotting have been proposed in the past, but they lack the structural detail necessary to capture important trotting behaviors such as back and neck flexion and aerial limb retraction (McMahon 1985; McMahon and Cheng 1990). Furthermore, the models did not include control systems. They described the mechanical behavior of the limbs and body during the stance period of a running gait. Those characteristics of body structure and limb movement that enable animals to run from cycle to cycle without falling over have not been examined.

The most noteworthy of these models was developed by McMahon and Cheng (1990). The model described limb stiffness and angle behavior during the contact phase of symmetric gaits such as quadrupedal trotting and bipedal running. In the trotting gait, a hindlimb strikes the ground close to the same time as a diagonal forelimb. These diagonal limb pairs were modeled with a single massless, undamped linear spring of stiffness, k_{leg}. The animal's total body mass was represented as a point mass attached to the top of the spring. McMahon and Cheng defined k_{leg} in terms of the peak vertical ground reaction force F_{max} acting at mid-stance when the leg spring is maximally compressed at a distance Δl, or

$$k_{leg} = \frac{F_{max}}{\Delta l}. \tag{A.1}$$

They defined a second stiffness, which they called the vertical stiffness, k_{vert}, to describe the vertical motions of the animal during the ground contact phase, or

$$k_{vert} = \frac{F_{max}}{\Delta y}, \tag{A.2}$$

where Δy is the distance the center of mass falls during the first half of ground contact. They also computed half the angle swept out by the leg spring during ground contact,

$$\theta_o = \sin^{-1}\left(\frac{ut_c}{2l_o}\right), \tag{A.3}$$

where l_o is the leg spring length at the instant of first ground contact, u is the forward velocity of the model, and t_c is the total time the leg spring is on the ground. Results describing animal stiffness, k_{leg}, k_{vert}, and limb excursion angle at first ground contact, $\grave{e}_o$ are plotted in Figure 7 for a 135 Kg trotting horse. These experimental results are compared to the predictions of the trotting horse model.

The Energetics of Trotting

Cross-bridge models of skeletal muscle are not used in this paper to predict directly the metabolic energy demands of quadrupedal running. Instead, an empirical rule is used to estimate energetic behavior using only mechanical predictions from the model. The empirical rule, presented by Kram and Taylor in 1990, is based on the observation that the reciprocal of limb contact time in running increases linearly with forward speed along with metabolic rate. A useful generalization can be found by dividing the weight-specific metabolic power by the reciprocal of an animal's limb contact time to get a cost coefficient that is largely independent of animal speed and size, or

$$\frac{P_{\text{met}}}{W} = \frac{C_o}{t_c}. \tag{A.4}$$

Here, P_{met} is the metabolic power required to run, W is body weight, t_c is the average time a leg remains in contact with the ground during a running cycle, and C_o is the proportionality constant or cost coefficient. For quadrupedal mammals, the cost coefficient has an approximate value of 0.2 J N^{-1} across both speed and size.

The metabolic cost of transport, the energy to transport unit weight a unit distance, can be found from eq. (A.4) by simply dividing by the animal's forward running speed, u, or

$$\text{Cost of Transport} = \frac{P_{\text{met}}}{W u} = \frac{C_o}{t_c u}. \tag{A.5}$$

In running simulations, the cost of transport is estimated by predicting how much time, on average, each limb of the trotting model remains on the ground at a particular forward speed u. Hence, in this paper, the Kram and Taylor rule serves as a bridge between the mechanics and energetics of locomotion.

References

Alexander, R. McN. 1977. Mechanics and scaling of terrestrial locomotion. In *Scale Effects in Animal Locomotion*, ed. T. J. Pedley, 93–110. New York: Academic Press.

Alexander, R. McN. 1985. Elastic structures in the back and their role in galloping in some mammals. *J. Zool. Lond. (A)* 207:467–482.

Bair, I. R. 1959. Amphibious walking vehicle. U.S. Patent number 2,918,738.

Biewener, A. A. 1989. Scaling body support in mammals: Limb posture and muscle mechanics. *Science* 245:45–48.

Cavagna, G. A., Heglund, N. C., and Taylor, C. R. 1977. Mechanical work in terrestrial locomotion: Two basic mechanisms for minimizing energy expenditure. *Am. J. Physiol.* 233:R243–R261.

Corson, P. E. 1958. Walking tractor. U.S. Patent number 2,822,878.

Ehrlich, A. 1928. Vehicle propelled by steppers. US Patent number 1,691,233.

Eyzaguirre, C., and Fidone, S. J. 1975. Physiology of the nervous system. 2d ed. Year Book Medical. Chicago, IL.

Farley, C. T., Glasheen, J., and McMahon, T. A. 1993. Running springs: Speed and animal size. *J. Exp. Biol.* 185:71–86.

Fedak, M. A., Heglund, N. C., and Taylor, C. R. 1982. Energetics and mechanics of terrestrial locomotion II. Kinetic energy changes of the limbs and body as a function of speed and body size in birds and mammals. *J. Exp. Biol.* 79:23–40.

Frank, A. A. 1970. An approach to the dynamic analysis and synthesis of biped locomotion machines. *Medical and Biological Engineering* 8:465–476.

Gray, J. 1968. *Animal Locomotion*. London: Weidenfeld & Nicolson.

Gubina, F., Hemami, H., and McGhee, R. B. 1974. On the dynamic stability of biped locomotion. *IEEE Trans. Biomedical Engineering BME* 21:102–108.

Heglund, N. C., and Taylor, C. R. 1988. Speed, stride frequency and energy cost per stride: How do they change with body size and gait? *J. Exp. Biol.* 138:301–318.

Herr, M. H. 1998. *A Model of Mammalian Quadrupedal Running*. Ph.D. thesis, Harvard University, Department of Biophysics.

Hoyt, D. F., and Taylor, C. R. 1981. Gait and the energetics of locomotion in horses. *Nature* 292:239–240.

Kinch, E. A. 1928. Vehicle propelling device. U.S. Patent number 1,669,906.

Kram, R., and Taylor, C. R. 1990. Energetics of running: A new perspective. *Nature* 346:265–267.

Lucas, E. 1894. Huitieme recreation—la machine a marcher. *Recreations Mathematiques* 4:198–204.

Manter, J. 1938. Dynamics of quadrupedal walking. *J. Exp. Biol.* 15:522–539.

McGeer, T. 1989. Passive bipedal running. Technical report CCS-IS TR 89-02, Simon Fraser University.

McGeer, T. 1990. Passive dynamic walking. *Int. J. Robotics Research* 9(2):62–82.

McGhee, R. B., and Kuhner, M. B. 1969. On the dynamic stability of legged locomotion systems. In *Advances in External Control of Human Extremities*, ed. M. M. Gavrilovic and A. B. Wilson, Jr, 431–442. Belgrade: Jugoslav Committee for Electronics and Automation.

McMahon, T. A. 1985. The role of compliance in mammalian running gaits. *J. Exp. Biol.* 115:263–282.

McMahon, T. A., and Cheng, G. C. 1990. The mechanics of running: How does stiffness couple with speed? *J. Biomech.* 23:65–78.

Miura, H., and Shimoyama, I. 1980. Computer control of an unstable mechanism. *J. Fac. Eng.* 17:12–13.

Miura, H., and Shimoyama, I. 1984. Dynamic walk of a biped. *Int. J. Robotics Research* 3:60–74.

Morrison, R. A. 1968. Iron mule train. *Proceedings of Off-Road Mobility Research Symposium, International Society for Terrain Vehicle Systems*, Washington, DC, pp. 381–400.

Muybridge, E. 1979. *Muybridge's Complete Human and Animal Locomotion*, vol. 3. New York: Dover.

Nilson, F. A. 1926. Supporting and propelling mechanism for motor vehicles. US Patent number 1,574,679.

Raibert, M. H. 1985. Four-legged running with one-legged algorithms. In *Second International Symposium on Robotics Research*, ed. H. Hanafusa and H. Inoue, 311–315. Cambridge, MA: MIT Press.

Raibert, M. H. 1986. *Legged Robots That Balance*. Cambridge, MA: MIT Press.

Raibert, M. H. 1990. Trotting, pacing and bounding by a quadrupeded robot. *J. Biomech* 23, suppl 1: 79–98.

Ringrose, R. 1997. *Self-Stabilizing Running*. Ph.D. thesis, MIT, Department of EECS.

Roberts, T. J. 1995. *Running Economically: Form, Gait, and Muscle Mechanics*. Ph.D. thesis, Harvard University, Department of Organismal and Evolutionary Biology.

Roberts, T. J. 1997, February. Personal data collection.

Roberts, T. J., Marsh, R. L., Weyand, P. G., and Taylor, C. R. 1997. Muscular force in running turkeys: The economy of minimizing work. *Science* 275:1113–1115.

Rosenthal, D. E., and Sherman, M. A. 1986. High performance multibody simulations via symbolic equation manipulation and Kane's method. *Journal of Astronautical Sciences* 34(3):223–239.

Rygg, L. A. 1893. Mechanical horse. US Patent number 491,927.

Snell, E. 1947. Reciprocating load carrier. U.S. Patent number 2,430,537.

Urschel, W. E. 1949. Walking tractor. U.S. Patent number 2,491,064.

Vukobratovic, M. 1973. Dynamics and control of anthropomorphic active mechanisms. In *First Symposium on Theory and Practice of Robots and Manipulator Systems*, ed. A. Morecki, G. Bianchi, and K. Kedzior, 313–332. Amsterdam: Elsevier.

Vukobratovic, M., and Stepaneko, Y. 1972. On the stability of anthropomorphic systems. *Mathematical Biosciences* 14:1–38.